HHS Public Access

Author manuscript

Mol Psychiatry. Author manuscript; available in PMC 2024 January 11.

Published in final edited form as:

Mol Psychiatry. 2023 April ; 28(4): 1622–1635. doi:10.1038/s41380-022-01932-w.

AgRP neurons coordinate the mitigation of activity-based anorexia

Ames K. Sutton Hickey[1,✉], **Sean C. Duane**[1], **Laura E. Mickelsen**[1], **Eva O. Karolczak**[1], **Ahmed M. Shamma**[1], **Anna Skillings**[1], **Chia Li**[1], **Michael J. Krashes**[1,2,✉]

[1]Diabetes, Endocrinology, and Obesity Branch, National Institute of Diabetes and Digestive and Kidney Diseases (NIDDK), National Institutes of Health, Bethesda, MD, USA

[2]National Institute on Drug Abuse (NIDA), National Institutes of Health, Baltimore, MD, USA

Abstract

Anorexia nervosa (AN) is a debilitating and deadly disease characterized by low body mass index due to diminished food intake, and oftentimes concurrent hyperactivity. A high percentage of AN behavioral and metabolic phenotypes can be replicated in rodents given access to a voluntary running wheel and subject to food restriction, termed activity-based anorexia (ABA). Despite the well-documented bodyweight loss observed in AN human patients and ABA rodents, much less is understood regarding the neurobiological underpinnings of these maladaptive behaviors. Hunger-promoting hypothalamic agouti-related peptide (AgRP) neurons have been well characterized in their ability to regulate appetite, yet much less is known regarding their activity and function in the mediation of food intake during ABA. Here, feeding microstructure analysis revealed ABA mice decreased food intake due to increased interpellet interval retrieval and diminished meal number. Longitudinal activity recordings of AgRP neurons in ABA animals exhibited a maladaptive inhibitory response to food, independent of basal activity changes. We then demonstrated that ABA development or progression can be mitigated by chemogenetic AgRP activation through the reprioritization of food intake (increased meal number) over hyperactivity, but only during periods of food availability. These results elucidate a potential neural target for the amelioration of behavioral maladaptations present in AN patients.

✉**Correspondence** and requests for materials should be addressed to Ames K. Sutton Hickey or Michael J. Krashes. amy.sutton@nih.gov; michael.krashes@nih.gov.

AUTHOR CONTRIBUTIONS

A.S.-H. and M.J.K. designed experiments. A.S.-H. and S.C.D. performed initial experiments in WT mice. A.S.-H., S.C.D., A.M.S., A.S. constructed FED3 devices used throughout experiments. A.S.-H., L.E.M. performed chemogenetic and photometry experiments. A.S.-H., E.O.K. performed behavioral experiments used in conjunction with ex vivo electrophysiology experiments. C.L. performed ex vivo electrophysiology experiments. A.S.-H., C.L. performed surgery for photometry experiments. A.K.S. performed analysis on all experiments. A.S.-H. and M.J.K. wrote the manuscript with input from S.C.D. and C.L.

COMPETING INTERESTS

The authors declare no competing interests.

Supplementary information The online version contains supplementary material available at https://doi.org/10.1038/s41380-022-01932-w.

INTRODUCTION

Anorexia nervosa (AN) is a global psychiatric disease primarily defined by decreased food intake and low bodyweight [1]. A key neurobiological feature of AN is the reversal of satiety's reinforcement value. In healthy individuals, hunger signals a negative valence, which is only relieved upon food consumption. Conversely, AN patients prefer a state of caloric deficiency over sated conditions, and food intake is often aversive [2–6]. Current therapeutic strategies for AN patients are primarily behavioral, as no FDA-approved medications exist for the condition, and severe cases oftentimes require forced feeding during prolonged involuntary hospitalization [7–10]. Given the aversive nature of food intake in AN patients, it is perhaps no surprise that relapse rates (~50%) are among the highest of any psychiatric illness; AN is also one of the most lethal psychiatric illnesses, with a standardized mortality ratio around 6 [11]. Moreover, AN is more commonly diagnosed in females [12–14]. Thus, there is a need for therapeutic alternatives that target the basic biology of AN.

Strikingly, a large proportion (up to 80%) of AN patients also display hyperactivity, due to excessive exercise and/or general restlessness [15–18]. A number of these key features of AN, including sex differences [19], can be replicated in the activity-based anorexia (ABA) rodent model, whereby some animals voluntarily become hyperactive in contexts of food restriction [20–22]. This leads to rapid health deterioration and ultimately death absent experimental intervention. Like humans displaying AN, ABA rodents over-expend energy, potentially due to an excessive drive to forage in contexts of deprivation [22, 23]. Additional hypotheses suggest that exercise during ABA becomes positively reinforcing, potentially relieving the negative effect of hunger [21, 24]. Yet, few studies have been able to untangle the neural representation of feeding during ABA, and even fewer have identified neural targets for the amelioration of this disease.

Allelic variability at the level of Agrp, the gene encoding hunger-promoting agouti-related peptide (AGRP) peptide in neurons of the arcuate nucleus (ARC), has been identified as a risk factor for AN in humans [25, 26]. Surprisingly, plasma AGRP levels are elevated in AN patients, and this is recapitulated at the mRNA and protein level in rodents demonstrating ABA [27–31]. Further complicating matters, chronic intracerebroventricular AGRP infusion ameliorates ABA by increasing feeding and decreasing hyperactivity in rats [30, 32].

AgRP neurons promote robust food seeking and subsequent food intake across a variety of environmental and physiological conditions [33–38]. Furthermore, AgRP neurons are inhibited during the sensory detection of food and remain durably suppressed following caloric intake in hungry mice [39–41]. This suppression has also been reported following bouts of exercise [39, 40, 42–44]. Interestingly, activation of AgRP neurons in adolescent mice during ABA without food present further promotes hyperactivity, yet somewhat paradoxically improves survival, while ablation exacerbates death [44]. Yet, it is unknown whether AgRP activation during contexts of food availability (and thus more similar to the behavioral choices made by AN patients) can alter ABA outcomes. It is possible that the elevation of AGRP levels during ABA might be the main driver of hyperactivity in contexts

devoid of food, and that the amelioration of ABA is dependent on specific AgRP activation timing.

We sought to clarify the role of AgRP neurons in ABA progression by first expanding our understanding of the behavioral abnormalities (particularly in feeding behavior) observed in mice displaying ABA. We then tested whether AgRP neurons appropriately respond to food retrieval in mice on the ABA paradigm. Finally, we studied the sufficiency and necessity of AgRP neurons in addressing the behavioral abnormalities underlying the excessive bodyweight loss observed in ABA mice, with a focus on probing and manipulating AgRP neurons across circadian time points with or without food access. To this end, we employed a combination of tools including multi-day, freely-moving in vivo fiber photometry and chemogenetic perturbations of AgRP neurons at discrete time periods. We discovered that AgRP population activity exhibits a dysregulated response to food specifically in ABA conditions, highlighting this population of neurons as a putative target for ABA maladaptive behavioral choice. Furthermore, artificial activation of AgRP neurons, only when food is available, relieves the excessive bodyweight loss observed during ABA by increasing meal number and overall food intake while reducing physical activity. Together, these findings suggest a potential therapeutic target for the relief of the hypophagia and hyperactivity observed in AN patients.

METHODS

Animals

C57BL/6 J, AgRP$^{tm1(cre)Lowl}$/J (stock no. 012899), R26-LSL-hM4Di (stock no. 026219), and R26-LSL-hM3Dq (stock no. 026220) mice were used. Mice were housed with a 12-h light/dark cycle and provided ad libitum access to food (standard chow, Envigo 7017 NIH-31, or 20 mg grain pellets, TestDiet 5TUM) and water, unless otherwise noted. All experiments were carried out in adult female mice that were group housed until experiments began. Some measurements were carried out in the same mouse across conditions (see individual methods sections for further details). All animal protocols and procedures were approved by the US National Institutes of Health Animal Care and Use Committee.

Behavioral paradigm

Mice were single housed and separated into one of three behavioral groups (Activity, FR, ABA) with ad libitum food access to food, water, and a voluntary wireless running wheel (Med Associates, ENV-047) in the unlocked (Activity, ABA) or locked (FR) configuration 3–5 days prior to the beginning of experiments. Beginning on Day 0, food was removed from FR and ABA mice 3 h after the start of the dark cycle. On all days following, food was provided for the first 3 h of the dark cycle. For mice in the Activity cohort, food was measured but not removed. Mouse bodyweights were measured immediately prior to the start of the dark cycle (before food presentation). Voluntary running behavior was initially collected and analyzed using Wheel Manager and Wheel Analysis (Med Associates), respectively. Some mice were resistant to the ABA or FR paradigm, as recently described across multiple rodent models [45–48]. To address this, we leveraged results from a recent study [45], suggesting that ABA and FR resistant mice lose on average ~12% (ABA) and

~14.5% (FR) of their original weight by Day 4. Mice were thus classified as resistant and removed from results (Figs. 1–2, 5 only) if they lost <12% (ABA) or <14.5% (FR) of their starting bodyweight by Day 4. All mice were habituated to i.p. Injections (100 uL saline) or fiber optic cord hookup for at least three days before the onset of the behavioral paradigm (Day 0), as appropriate. Resistant mice were removed from analyses as described above (Activity $n = 4$, FR-resistant $n = 6$, FR-susceptible $n = 1$, ABA-resistant $n = 5$, ABA-susceptible $n = 10$).

Food Intake from Feeding Experimentation Devices (FED3)

Feeding information was collected using FED3 devices, which dispense 20 mg pellets of chow food either ad libitum (Free Feed mode) or at predefined times (Timed Feed mode) [49]. Mice were habituated to the FED3 device in the homecage for at least one day with their normal standard chow on the ground of the homecage, afterwhich standard chow was removed and mice were exclusively fed from FED3 in Free Feed mode. Beginning on Day 0, the FED3 mode was changed to Timed Feed (FR/ABA mice only) and mice had food access from FED3 for 3 h at the beginning of the dark cycle. Pellet intake was measured across days of the ABA paradigm in FR and ABA mice using both cumulative and 15 min binned measurements. Pellets were classified as part of the same meal if they were retrieved within 148.2 s of another pellet (>1 pellet/meal requirement), which was the mean IPI for wildtype FR mice across Days 1–3.

Viral vectors

AAV1-hSyn-Flex-GCaMP6s (Addgene, 100845) was used for in vivo fiber photometry recordings of AgRP-expressing ARC neurons. AAV8-hSyn-Flex-mCherry (Addgene, 50459) and AAV8-hSyn-Flex-hM3Dq-mCherry (NIEHS) were used for experiments designed for chemogenetic activation of AgRP neurons.

Viral injections and optical fiber implants

Stereotaxic injections were performed as previously described [33]. Briefly, mice were anesthetized with isoflurane and placed in a stereotaxic frame (Stoelting's Just for Mouse) and provided with analgesia (meloxicam, 0.5 mg/kg). Following a small incision on top of the skull and skull leveling, a small hole was drilled for injection. A pulled-glass pipette (20–40 mm tip diameter) was inserted into the brain at coordinates aimed at the ARC (AP: −1.40, ML: +− 0.25), and 200 nL of virus was injected at two depths (DV: −5.75 and −5.65) using a micromanipulator (Grass Technologies, Model S48 Stimulator, 25 nL/min). For in vivo photometry experiments, an optic-fiber cannula (core=400 um; 0.48 NA; M3 thread titanium receptacle; Doric Lenses) was implanted directly over the ARC (AP: −1.40, ML: + 0.25, DV: −5.55) following virus injection, and fixed to the skull (C&B-Metabond Quick Adhesive Cement/dental acrylic). Mice were placed on a heating pad and allowed to recover before single housing mice until further experimentation (>2 weeks post-surgery).

In vivo fiber photometry set-up

To excite GCaMP6s, <20 uW blue LED light at 470 nm was driven by a multichannel hub (Thorlabs), modulated at 211 Hz, and subsequently delivered to a dichroic mini cube

(FMC5, Doric Lenses) that was connected with optic fibers and a rotary joint (FRJ 1 × 1, Doric Lenses) to the optic cranial implant of the mouse. GCaMP6s calcium GFP signals were collected through the same fibers and dichroic minicube into a Femtowatt Silicon Photoreceiver (2151, Newport). Digital signals were subsequently demodulated, amplified and collected through a lock-in amplifier (RZ5P, Tucker-Davis Technologies (TDT)). LED modulation and data collection were performed using Synapse (TDT).

Freely-moving in vivo fiber photometry screening

To test for comparable $AgRP^{GCaMP6s}$ expression, mice were screened for viral/optic fiber hits. Following an 18 h overnight fast, mice were hooked up to the fiber patch cord and allowed to habituate to the set-up in their homecage for ~3 min. Following two minutes of baseline recording, a pellet of standard chow diet was placed on the cage bottom, and recordings continued for ~2 min. Synchronized high-definition videos were recorded for time-locked data analysis in Synapse, which was downsampled to 8 Hz. Mice with missed viral and/or fiber targeting were removed from analyses ($n = 4$).

Freely-moving in vivo fiber photometry during ABA

At least one week following the initial screening experiments, mice were placed in one of three experimental cohorts (as described above) and housed in PhenoTyper cages (Noldus) containing a voluntary running wheel (locked, FR mice; unlocked, ABA and Activity mice), and a FED3 device. On Day 1 and Day 4, mice were hooked up to the fiber patch cord during the light cycle and allowed to habituate for at least one hour. Some mice were repeated across multiple cohorts to limit the number of total mice used in these experiments, with crossover across conditions to control for time effects and repeated measurements (repeated animals: ABA→Wheel → FR (n=1), Wheel→ABA→FRR ($n = 1$), Wheel→ABA ($n = 1$), FR→ABA ($n = 1$), total mice: Activity $n = 6$, FR $n = 6$, ABA $n = 7$). Recordings began at least 15 min prior to the dark cycle, allowing for detection of the first bout of feeding in FR and ABA mice. Pellet dispense and retrieval were determined by TTL pulses driven by FED3 that were time-locked to photometry recordings using Synapse. Recordings continued for one hour into the dark cycle, at which point recordings stopped and mice were unhooked from the fiber patch cord. Analysis was performed by downsampling recordings to 8 Hz and subsequently calculating perievent signals around pellet retrieval using NeuroExplorer (Plexon). Signals were normalized by z-score to the first 5 seconds of the recording (−10→−5s).

Ex vivo electrophysiology

NPY-hrGFP or AgRP-iCre, ZsGreen female mice of age 3-4 months were placed in one of three experimental cohorts (as described above) and housed in PhenoTyper cages (Noldus) containing a voluntary running wheel (locked, FR mice ($n = 4$); unlocked, Activity ($n = 4$) and ABA ($n = 5$) mice) and a FED3 device. About 30min prior to the dark cycle (when food would have been provided by FED3 for FR and ABA mice) on Day 1, mice were decapitated under isofluorane anesthesia Brains were rapidly removed and placed in ice-cold sucrose artificial cerebrospinal fluid (ACSF): (in mM) 194 sucrose, 20NaCl, 4.4KCl, 2CaCl2, 1MgCl2, 1.2NaH2PO4, 10.0 glucose, and 26.0NaHCO3 saturated with 95% O2/5% CO2. Three hundred micron slices were prepared using a Leica VT1000 vibratome (Wetzlar,

Germany). Brain slices containing the ARC were obtained and stored at approximately 30 °C for an hour in a heated, oxygenated holding chamber containing artificial cerebrospinal fluid (ACSF) (in mmol/L) 124NaCl, 4.0 KCl, 2 CaCl2, 1.2 MgSO4, 1 NaH2PO4, 10.0 glucose, and 26.0 sodium bicarbonate. They were then transferred to a submerged recording chamber maintained at approximately 30 °C (Warner Instruments, Hamden, Connecticut) for around 30 min before recording. Recording electrodes (2–5 MΩ) were pulled with a Flaming-Brown Micropipette Puller (Sutter Instruments, Novato, CA), using thin-walled borosilicate glass capillaries. Recording electrodes were filled with (in mmol/L) 130 K-gluconate, 10KCl, 0.3$CaCl_2$, 1$MgCl_2$, 1EGTA, 3MgATP, 0.3NaGTP, 10Na-phosphocreatine, and 10 Hepes, pH = 7.35 with KOH, 291 mOsmol. All experiments were conducted under the current clamp configuration. Rheobase experiments were conducted while injecting negative current to maintain the membrane potential at −70 mV, then positive current ramps were applied to acquire current needed for the first action potential. Signals were acquired via a Multiclamp 700B amplifier (Molecular Devices, Sunnyvale, California), digitized at 20 kHz, filtered at 3 kHz, and analyzed using Clampfit 10.11 software (Molecular Devices). Experiments in which changes in access resistance were greater than 20% before and after the experiments were not included in the data analysis.

AgRP 3Dq screening

Following surgery recovery, $AgRP^{mCh}$ and $AgRP^{3Dq}$ mice were injected with either vehicle (1U/g BW, 10% β-cyclodextrin) or clozapine n-oxide (CNO; 1 mg/kg in 10% β-cyclodextrin) in a crossover design and given access to a pre-measured pellet of standard chow. Food intake was measured one hour after injection. Mice with missed viral targeting were removed from analyses ($n = 4$).

AgRP activation experiments - Days 1–7 (light and dark cycle)

At least one week following screening experiments, $AgRP^{mCh}$ and $AgRP^{3Dq}$ mice were separated into one of three groups (Activity, FR, ABA). Beginning on Day 0, all mice were injected with vehicle (Day 0; 1U/g BW, 10% β-cyclodextrin) or CNO (Days 1–7; 1 mg/kg) 15 min before the onset of the dark cycle (Fig. 4) or at the onset of the light cycle (Supplementary Fig. 1). To limit the use of total mice used, some mice in these experiments were used previously in other AgRP activation experiments (light cycle: ABA-3Dq $n = 1$; total mice - dark cycle: Activity-mCh $n = 6$; Activity-3Dq $n = 7$; FR-mCh $n = 7$; FR-3Dq $n = 7$; ABA-mCh $n = 8$; ABA-3Dq $n = 8$; total mice - light cycle: Activity-mCh $n = 6$; Activity-3Dq $n = 7$; FR-mCh $n = 7$; FR-3Dq $n = 7$; ABA-mCh $n = 8$; ABA-3Dq $n = 8$).

AgRP activation experiments - Days 4–7

$AgRP^{mCh}$ and $AgRP^{3Dq}$ mice were all placed on the ABA behavioral paradigm, with food access provided by FED3 devices. All mice were injected with either vehicle (Days 0, 1, 2, 3; 10% β-cyclodextrin) or CNO (Days 4, 5, 6, 7; 1 mg/kg) ~15 min prior to the onset of the dark cycle. To limit the use of total mice used, some mice in these experiments were used previously in other AgRP activation experiments (ABA-mCh: $n = 4$, ABA-3Dq: $n = 6$). Resistant mice were removed from analyses as described above (ABA-mCh-resistant $n = 3$, ABA-mCh-susceptible $n = 8$, ABA-3Dq-resistant $n = 1$, ABA-3Dq-susceptible $n = 11$).

AgRP inhibition experiments

AgRP^{cont} and AgRP^{hM4Di} mice were pre-screened with a fast-refeed experiment, in which mice were fasted overnight (14–16 h), and then injected with either vehicle or CNO (3.0 mg/kg) ~1 h into the onset of the light cycle. One hour later, food was provided and two-hour food intake was measured. Mice were counterbalanced and given at least 3 days in between experiments to recover. At least one week following screening, mice were placed in one of the three behavioral cohorts, with food access provided by FED3 devices (Activity-control $n = 6$; Activity-4Di $n = 5$; FR-control $n = 5$; FR-4Di $n = 7$; ABA-control $n = 6$; ABA-4Di $n = 6$). One hour before the dark cycle began (when food was available for FR/ABA mice), mice were injected with either vehicle (Day 0; 10% β-cyclodextrin) or CNO (Days 1–3; 3 mg/kg in 10% β-cyclodextrin).

Perfusion and histology

Following experiment completion, mice with viral injections were terminally anesthetized using chloral hydrate (Sigma-Aldrich) and transcardially perfused first with phosphate-buffered saline (PBS) followed by 10% neutral buffered formalin (Fisher Scientific). Brains were removed, post-fixed, and dehydrated in 30% sucrose before sectioning into 30–50 um slices using a freezing sliding microtome (Leica Biosystems). Coronal sections were collected and stored at 4 °C. Slices were mounted with a mounting medium containing DAPI (Vectashield) and images were captured using a 10X objective on a Zeiss Observer Z1 confocal microscope.

Statistical analysis

All post-data collection analyses were performed in R Studio. Paired *t*-tests, unpaired t-tests, one-way ANOVAs followed by Tukey post-hoc tests (if applicable), two-way ANOVAs followed by Bonferroni post-hoc tests (if applicable), or two-way mixed ANOVAs followed by Bonferroni post-hoc tests (if applicable) were calculated as appropriate. Normality and homogeneity of variances were tested and, if necessary, accounted for using the Shapiro-Wilk and Levene's tests, respectively. Significance was determined for $p < 0.05$.

RESULTS

Food Restriction with voluntary running wheel access exacerbates negative energy balance

Numerous studies have demonstrated that bodyweight loss occurs in rodents in contexts of time-restricted food access in combination with a running wheel to varying degrees [20, 21, 45, 50, 51]. To recapitulate this behavioral paradigm, we placed wildtype (WT) mice in one of three cohorts: Activity, Food Restricted (FR), or Activity-Based Anorexia (ABA). Activity mice were provided ad libitum food throughout the experiment in conjunction with a functional running wheel (thus serving as a control for voluntary wheel running activity, Fig. 1a). A separate control cohort consisted of FR mice that were granted 3 hr daily food access at the onset of the dark cycle and provided with a locked running wheel in their homecage (Fig. 1b). To measure the effects of both voluntary wheel running and food

restriction, ABA mice were provided with a running wheel and were food restricted for the same length as FR mice, beginning on Day 0 of the paradigm (Fig. 1c).

Like previous studies, mice in the Activity cohort maintain their bodyweight over the course of the paradigm, whereas FR causes mice to lose weight that stabilizes after Day 3 (Fig. 1d, e). In comparison, ABA mice exhibit weight loss that is more profound than FR mice (Fig. 1d). While FR and ABA mice both increase feeding during 3-hour food access over the course of the paradigm (two-way ANOVA, effect of time, Fig. 1f), ABA mice eat less than FR mice (Fig. 1g). Since Activity mice are provided ad libitum food, food intake in Activity mice is less than FR and ABA mice during the first three hours of the dark cycle, whereas daily food intake is higher in Activity mice than either FR or ABA cohorts (Fig. 1h, i). This suggests that Activity mice maintain bodyweight by matching energy input with output, whereas ABA mice are unable to maintain bodyweight, at least in part due to diminished food intake relative to FR controls.

In concert with food intake analyses, we investigated the voluntary wheel running activity in Activity and ABA mice. Although ABA mice are food restricted and losing bodyweight, their total wheel running activity is neither different from ad libitum fed Activity controls (Fig. 1j, l) nor different from baseline conditions in which food was provided ad libitum within the same mice (Fig. 1k). Similarly, despite food availability only during the first three hours of the dark cycle for ABA mice on Days 1–3, running during this time period does not significantly diminish compared to Activity mice until Day 3 of the paradigm, after which mice have lost significant bodyweight (Fig. 1m). The majority of time spent wheel running in Activity mice was during the dark cycle, when mice are typically more active, and ABA mice ran a similar amount as Activity mice during this time period (Fig. 1p, r), as well as similar levels as during baseline conditions (Fig. 1q). Surprisingly, ABA mice ran significantly more during the light cycle when compared to baseline levels (Fig. 1t), a period when Activity mice run on the wheel very little (Fig. 1s, u). Similar to previous reports across rodent models of ABA [45, 46, 52–54], ABA mice also increased running during the hour before food availability (termed Food Anticipatory Activity, FAA) when compared to baseline levels, whereas mice in the Activity cohort did not significantly differ in FAA (Fig. 1v, x). This suggests that despite sustained bodyweight loss due to hypophagia, ABA mice voluntarily engage in wheel running activity at comparable (and sometimes elevated) levels as ad libitum fed mice.

ABA mice have dysregulated feeding behavior

Previous studies interrogating the role of maladaptive feeding in ABA progression have been inconclusive, potentially due to different behavioral paradigms (e.g., methodology of food intake measurement, length and/or circadian timing of food availability) [30, 44–46, 55]. We suspected that this was also, at least in part, due to the fact that food intake is oftentimes more nuanced than a finalized measurement of total intake. To address this limitation, we used a Feeding Experimentation Device (FED3), designed to accurately measure food intake by dispensing 20 mg grain pellets and recording mouse retrieval (Fig. 2a, b) [49]. With this qualitative and quantitative approach, we demonstrate with more specificity the timepoints that ABA mice differ in their cumulative food intake in comparison to FR controls. ABA

mice ate at a slower rate than FR controls, thus contributing to decreased total intake over time (Fig. 2c). Utilizing this approach, we were also able to calculate the frequency with which mice obtained a pellet from the FED3 over the course of the experiment (Fig. 2d, e). ABA mice appeared to have fewer bouts of feeding in comparison to FR mice on food restricted days. Thus, we hypothesized that FR and ABA mice might differ in meal patterns.

To accurately detect meal size and meal number, we first measured the interpellet interval (IPI) in both cohorts of mice. (f-g) The kernel density estimation (KDE) IPI peak (~30 s) for FR mice is maintained across Days 1–3, suggesting that mice do not significantly alter how frequently they retrieve pellets over the course of multiple days of food restriction (Fig. 2f). In contrast, IPI KDE curves in ABA mice shift to the right on Day 2-3, suggesting more frequent increases in between each individual pellet retrieval as the behavioral paradigm progresses (Fig. 2g). Since KDE curves in FR mice indicate that the majority of pellets were consumed with an IPI < 30 sec, we measured the percentage of pellets eaten with an IPI < 30 sec or ≥30 sec in FR and ABA mice across days (Fig. 2h–j). While FR mice do not alter the percentage of pellets eaten with an IPI < 30 sec (Fig. 2h–j) or ≥30 sec (Fig. 2i, j) from Day 1–3 of the paradigm, ABA mice display a shift in their food intake patterns whereby the percentage of pellets with an IPI < 30 s or ≥30 s trends downward and upward, respectively (Fig. 2h–j). These analyses demonstrate that ABA mice consume lower amounts of food than FR mice due to increased duration in between individual pellet retrieval.

Meal number is decreased in ABA mice

Since IPI analyses (Fig. 2f–j) suggested that ABA mice alter IPI timing, we investigated whether this was reflected in meal number or meal size in ABA mice compared to FR controls. While KDE peaks were observed with an IPI ~30 s on Day 1 across groups, we intended to determine meals based on the mean IPI of pellet consumption across all days of food restriction in FR mice (~IPI ≤ 148.2s, Fig. 2k). Using this approach, we were able to visualize and measure the number of meals initiated by FR or ABA mice (Fig. 2l, m). While ABA and FR mice demonstrated similar meal sizes (Fig. 2n), ABA mice had fewer meals than FR controls (Fig. 2o). Furthermore, the latency to begin the first meal was higher in ABA mice compared to FR controls upon food restriction (Fig. 2p, q). This suggests that ABA mice have decreased feeding due to fewer meal initiations rather than altering the amount of intake after a meal has begun and highlights a behavioral distinction in ABA mice that potentially drives bodyweight loss.

Feeding-induced AgRP inhibition is dysregulated in ABA mice

We next sought to identify a potential neural circuit capable of mediating food intake that might underlie the deficiency in food acquisition (and subsequent consumption) that we observed in ABA mice. AgRP neurons in the ARC have been well characterized for their ability to sense energy status via peripheral hormones and subsequently promote food intake across satiety conditions [33–35, 56, 57]. Given that AgRP neurons are well described to regulate food intake, we assessed AgRP activity during feeding across ABA progression.

To measure the response of AgRP neurons to feeding across behavioral conditions, we used in vivo fiber photometry in freely behaving AgRP-iCre mice (Fig. 3a–c). Before assigning

mice to specific groups, we performed a baseline screening experiment aimed at testing injection and fiber placements during a fast-refeed (Fig. 3e). As observed previously, AgRP neurons were rapidly inhibited in response to food presentation in the fasted state [39, 40, 58], and this response was similar across all mice that were subsequently divided into one of three behavioral groups (Activity, FR, ABA; Fig. 3g, h, top). This suggests that any differences observed in response to food intake during the behavioral paradigms are not due to targeting differences.

Photometry recordings were performed before the start of the dark cycle (when food was available for FR and ABA mice) on Day 1 and Day 4 (Fig. 3f). This analysis demonstrates that food intake significantly decreased AgRP activity in FR mice in comparison to ad libitum fed Activity controls following one day of food restriction in FR mice; this inhibition was absent in ABA mice (Fig. 3g, h, middle). While feeding-induced AgRP inhibition in FR mice continued on Day 4 of food restriction, the lack of inhibition seen on Day 1 in ABA mice was no longer observed (Fig. 3g, h, bottom). This suggests that food intake-induced AgRP inhibition is disrupted at the beginning of ABA, since AgRP activity in ABA mice is more similar to that of ad libitum fed Activity mice than animals in a negative energy state (FR). Moreover, these results suggest that AgRP inhibition in response to food intake in ABA mice is restored by Day 4 of the paradigm, at a time point in which ABA mice have lost significantly more bodyweight than FR mice.

Basal measures of AgRP neuronal activity is unaltered in ABA mice

Since feeding-mediated AgRP neuronal inhibition in response to food deprivation was blunted in ABA mice, it is possible that the basal activity of AgRP neurons was decreased in ABA mice, thus decreasing the capability of these neurons to be inhibited upon food consumption. To test this, we performed ex vivo electrophysiology in AgRP neurons from mice on the Activity, FR or ABA paradigm immediately prior to the onset of the dark cycle (i.e. prior to food availability in FR/ABA mice; Fig. 3i). Importantly, we performed these experiments on Day 1 of the experimental paradigm, a time point when we observed a lack of feeding-induced AgRP inhibition in mice on the ABA paradigm. We observed no differences in basal measurements of neuronal activity, including firing rate (Fig. 3j), membrane capacitance or resistance (Fig. 3k, l), or rheobase (Fig. 3m). Additional analyses performed exclusively on firing neurons further demonstrated that the basal cellular activity of AgRP neurons was unchanged across Activity, FR, and ABA mice (Supplementary Fig. 1). Taken together, these results suggest that the absence of feeding-mediated inhibition in AgRP neurons observed in ABA mice is not due to a basal change in activity in these cells.

Chemogenetic AgRP activation ameliorates bodyweight loss in ABA mice

Artificial AgRP activation, using either chemogenetic or optogenetic approaches, increases food intake in rodents across multiple behavioral contexts [33–37, 59–61]. Feeding-induced AgRP neuronal inhibition was dysregulated in ABA mice, raising the possibility that food intake in ABA mice does not relieve the negative valence associated with AgRP neuronal activation. We posited that this continued aversion prevents future food intake. Thus, we sought to determine if stimulating AgRP neuronal activity could alleviate ABA development by driving food seeking. To achieve this, we expressed hM3Dq (3Dq), a designer receptor

exclusively activated by designer drugs (DREADDs) in AgRP neurons using AgRP-iCre mice and compared them to littermate controls or mice injected with a control fluorophore (Fig. 4a, b). First, we successfully validated that 3Dq-mediated AgRP activation reliably drives feeding behavior in sated mice before experiments began (Fig. 4c).

To test the effect of chemogenetic activation of AgRP neurons in ABA progression, each cohort of mice had both a control (mCh) and experimental sub-cohort (3Dq). All mice were administered vehicle on Day 0 of the paradigm 15 min prior to the onset of the dark cycle, whereas CNO was administered on Days 1–7 in all cohorts (Fig. 4d). Using this approach, we were able to decipher the effect of artificial AgRP stimulation in ad libitum fed Activity mice (Activity-mCh vs. Activity-3Dq), FR mice (FR-mCh vs. FR-3Dq), and ABA mice (ABA-mCh, ABA-3Dq). Indeed, activation of AgRP neurons increased bodyweight in ad libitum fed Activity (Fig. 4e, purple), FR (Fig. 4e, green) and ABA (Fig. 4e, yellow) mice.

Since we initially determined that bodyweight loss is at least partly due to a reduction in food intake in ABA mice, we investigated if food intake was altered in AgRP-3Dq mice compared to their respective AgRP-mCh controls. While no change was observed in food intake on Day 0 (pre-AgRP activation, Fig. 4f, i), significant increases in food intake were observed in Activity-3Dq, FR-3Dq and ABA-3Dq mice in comparison to their mCh control cohorts when CNO was administered (Fig. 4g, h, j, k). These results suggest that ABA bodyweight reversal as a result of AgRP activation is due, at least in part, to increased food intake.

Our initial behavioral tests suggested that voluntary wheel running activity in contexts of food restriction is likely a contributing factor to the bodyweight loss observed in ABA mice. Thus, we investigated how chemogenetic AgRP activation alters voluntary wheel running activity in ad libitum fed and food deprived conditions in Activity and ABA mice, respectively. Total voluntary running activity in Activity-3Dq and ABA-3Dq mice was unaltered in response to vehicle (Fig. 4l) or CNO (Fig. 4m, n) injections in comparison to Activity-mCh and ABA-mCh controls, respectively. Further analyses of voluntary wheel running demonstrated that no measurement of voluntary wheel running was altered in response to CNO-mediated AgRP activation in Activity or ABA conditions (Supplementary Fig. 2). Together, these results suggest that AgRP activation across behavioral contexts (ad libitum food with a running wheel, food restriction without a running wheel, food restriction with a running wheel) increases bodyweight primarily due to increased food intake.

Artificial AgRP activation without food available does not alter bodyweight in ABA mice

To further define the circadian timepoint necessary for AgRP-mediated ABA amelioration in adult mice, we activated AgRP neurons during food availability, with both control (Activity-cont, FR-cont, ABA-cont) and experimental (Activity-3Dq, FR-3Dq, ABA-3Dq) cohorts (Supp Fig. 3a). We determined that AgRP activation during the light cycle over the course of multiple days did not affect bodyweight in Activity, FR or ABA conditions (Supplementary Fig. 3d). While AgRP activation during the light cycle is able to drive feeding in ad libitum fed Activity mice (Supplementary Fig. 3e, f, purple), this is not sustained during the dark cycle (Supp Fig. 3g, h, purple). AgRP activation during the light cycle does not affect dark cycle feeding in FR or ABA conditions (Supplementary Fig. 3g–j; green and yellow,

respectively), likely because CNO's ability to promote AgRP activity has substantially diminished 12 h after administration (CNO half-life = 8 h [62]).

Since AgRP activation has been shown to promote hyperactivity in conditions without food access, we hypothesized that ABA-3Dq mice would demonstrate enhanced wheel running during the light cycle, thereby underlying the inability for activation at this timepoint to promote ABA resilience. While AgRP activation did not alter running behavior across all measured timepoints in Activity conditions (Supp Fig. 3k–r), CNO administration increased light cycle wheel running in ABA-3Dq mice compared to ABA-controls (Supplementary Fig. 3k), without significantly affecting dark cycle running, running during food availability, total wheel running, or food anticipatory wheel running (Supplementary Fig. 3m–t). These results demonstrate that AgRP activation is capable of promoting feeding behavior over hyperactivity during the inactive light cycle when food is provided ad libitum (i.e., Activity conditions). However, light cycle AgRP activation without food present in ABA conditions promotes hyperactivity without changing subsequent dark cycle feeding.

AgRP inhibition prior to food availability increases bodyweight loss in FR and ABA mice

AgRP neuronal inhibition in response to food consumption in hungry mice is hypothesized to reflect an animal's re-calculation of food availability, and subsequently decrease their hunger level. Indeed, AgRP neurons are necessary for feeding behavior in varying energy balance states. Yet, the relevance of decreased AgRP neuronal activity specifically during food availability in adult mice on the ABA paradigm is unknown. To fill in this gap, we aimed to test if AgRP neurons are necessary for bodyweight maintenance in ABA mice using acute chemogenetic silencing of AgRP neurons during food availability.

One major limitation of artificial inhibition experiments to date lies in the necessity to achieve complete penetration of the inhibitory receptor/opsin in the population of interest. We leveraged the fact that AgRP neurons reside exclusively in the ARC, by utilizing a genetic approach (rather than viral) to express hM4Di in all AgRP neurons, with AgRP-iCre, R26-LSL-hM4Di mice (Supplementary Fig. 4a) [63]. Similar to previous reports [33], AgRP inhibition one hour prior to food presentation in fasted mice is sufficient to decrease food consumption (Supplementary Fig. 4b), validating this approach for use in ABA conditions.

We aimed to test the effect of AgRP inhibition across all behavioral cohorts (Activity, FR and ABA), and thus each cohort had both a control ("cont") and experimental (hM4Di, "4Di") condition (Supplementary Fig. 4c). While multi-day inhibition of AgRP neurons via CNO injection does not alter bodyweight in Activity mice, AgRP inhibition enhances the bodyweight loss observed in response to food deprivation both with or without a running wheel present (Supplementary Fig. 4d). AgRP inhibition in Activity mice does not alter ad libitum food intake (Supplementary Fig. 4e–h). Surprisingly, AgRP inhibition across all behavioral conditions does not suppress food intake (Supplementary Fig. 4e–h). While AgRP inhibition does not alter total running in Activity mice, acute AgRP silencing in ABA conditions causes increased running compared to ABA controls (Supplementary Fig. 4i, j), without affecting food anticipatory activity on the running wheel (Supplementary Fig. 4k, l). These results propose that AgRP inhibition during food availability is necessary for bodyweight maintenance exclusively in response to food deprivation, despite not

significantly altering food intake. Moreover, when food deprivation is paired with access to a voluntary running wheel (i.e. ABA conditions), AgRP inhibition exacerbates bodyweight loss at least partially due to increased voluntary running behavior.

Chemogenetic AgRP neuronal activation nullifies ABA progression

Although our initial chemogenetic experiments were aimed to test the preventative capabilities of AgRP activation on ABA development, this approach has limited translational potential since most individuals exhibit ABA before intervention is possible. To test the capability of AgRP neuronal activation to rectify ABA, we performed AgRP activation after ABA progression had begun and mice had already lost significant bodyweight. Following initial vehicle injections on Days 0–3, ABA-mCh and ABA-3Dq mice received CNO injections, thereby activating AgRP neurons in ABA-3Dq mice following initial bodyweight loss (Fig. 5a, b). While ABA-mCh and ABA-3Dq mice did not differ in their initial bodyweight loss during vehicle injections, CNO administration in ABA-3Dq mice beginning on Day 4 was capable of rapidly and robustly improving bodyweight loss compared to ABA-mCh controls (Fig. 5c). This amelioration was partially due to decreased total and dark cycle wheel running in comparison to vehicle-injected days (Fig. 5d, g, ABA-3Dq). In contrast, all measurements of wheel running activity were unchanged between CNO and vehicle injection days in ABA-mCh mice (Fig. 5d–h, ABA-mCh).

AgRP-activation in ABA mice also increased food intake compared to ABA-mCh controls on the first day of CNO administration (Fig. 5i, Day 4). This suggests that the bodyweight increase in ABA-3Dq mice is due to both decreased wheel running activity and increased food consumption.

Chemogenetic AgRP neuronal activation modifies meal number deficiencies in ABA mice

Our initial experiments uncovered that ABA mice initiate fewer meals than FR controls, thus highlighting a potential behavioral intervention method of increasing food intake in ABA conditions. To assess if AgRP activation-induced ABA amelioration was in part due to altered meal patterns, we further analyzed feeding data from FED3 devices used by ABA-mCh and ABA-3Dq mice in response to vehicle (Days 0–3) or CNO injections (Days 4–7). Indeed, binned pellet intake was increased upon the initiation of feeding in ABA-3Dq mice when CNO was administered by Days 5–7 of the paradigm (Fig. 5j). While meal size was unaltered in response to AgRP activation (Fig. 5l), CNO administration in ABA-3Dq increased meal number compared to ABA-mCh mice (Fig. 5n). These findings demonstrate that artificial AgRP activation reverses the meal number deficiency characterized by ABA, thus contributing to a rescue of ABA progression.

DISCUSSION

Studies have emphasized the behavioral complexities of ABA, and more recent reports have begun to unravel the neurobiology potentially underlying ABA [31, 44, 45, 50, 51, 64, 65]. Despite these advances, no study to date has identified a neural circuit capable of combating ABA development and/or progression by addressing both anorexia and hyperactivity. Here, we highlight the ability of AgRP neurons to override these maladaptive behaviors and

subsequently coordinate bodyweight maintenance and survival. We first identify the feeding microstructure in mice displaying ABA and highlight meal number as the main feeding deficiency in ABA mice. We also demonstrate that AgRP neuronal inhibition in response to food intake is impaired in ABA mice, such that AgRP dynamics more closely resemble ad libitum fed conditions than animals in caloric deficit. We subsequently addressed these abnormalities in ABA mice using chemogenetic activation of AgRP neurons throughout ABA, and were able to alleviate ABA bodyweight loss via increased feeding. Finally, we demonstrate that AgRP activation is capable of mitigating ABA following the initial progression of bodyweight loss via increased food intake and decreased wheel running. Importantly, the reversal of ABA by AgRP activation is performed during food availability, clarifying the capability of AgRP neurons to promote food intake when activation is performed during a more physiologically relevant time (i.e. when endogenous AgRP neuronal activity is elevated).

AgRP activation in contexts without food is aversive; this negative valence associated with heightened AgRP activity is relieved upon food intake in healthy individuals [35, 42]. While fasting-induced AgRP neuronal inhibition has been well documented in response to less than one day of fasting, no studies have demonstrated the effect of multi-day food restriction on AgRP neuronal activity. Here, we demonstrate that AgRP neurons are appropriately inhibited during food intake following one or four days of food restriction. However, this inhibition is lost in contexts with voluntary wheel running, suggesting that feeding-induced AgRP neuronal inhibition more closely resembles a sated state during ABA. Importantly, we highlight that this alteration is not due to a change in the basal activity of AgRP cells prior to food access in ABA mice, implicating that this disruption is an acute response to food intake in ABA conditions. Moreover, these results suggest that the blunted response of AgRP activity in response to food consumption in ABA mice is transient, since the loss of inhibition observed in ABA mice is no longer detectable by Day 4 of the behavioral paradigm. Taken together, these results suggest that AgRP activity is primarily dysregulated in food-related contexts at the beginning of food restriction in contexts with a voluntary running wheel, which might explain why ABA individuals demonstrate reduced food intake predominantly during the first few days of food restriction. Additional studies would be required to determine if this decrease in AgRP neuronal responsivity to food on the first day of food restriction is a predictive measure for ABA outcomes.

These results are similar to the decreased inhibition of AgRP neurons observed in response to presentation of normal chow following exposure to an obesogenic diet [66, 67]. Yet, in diet-induced obesogenic states, AgRP stimulation-induced standard chow intake is significantly blunted, whereas activation of AgRP neurons in ABA conditions strongly promotes chow intake. Thus, the capability of AgRP activation to trigger food intake is uniquely tailored to non-positive energy balance states. Future studies are needed to determine if midbrain dopaminergic circuits, which are altered by both ABA and high-fat diet exposure, mediate AgRP's divergent ability to drive feeding amidst shifting energy balance states [50, 67–70]. Additionally, since bodyweight loss, as observed in both FR and ABA mice, triggers a substantial reduction in body temperature, it is plausible that the effects we observed have identified a role of AgRP neurons in restoring body temperature in negative energy balance. Indeed, AgRP activation in FR conditions without a running wheel

present were also capable of restoring bodyweight. Future studies are required to determine the contribution of decreased body temperature in AgRP-mediated bodyweight restoration in states of negative energy balance.

While AgRP neurons have been well described for their ability to both sense peripheral energy signals and subsequently drive feeding behavior, few studies have measured their capability to coordinate maladaptive anorexic behaviors [33–35, 41, 71]. AgRP neurons are necessary for feeding (and subsequent survival) in adult mice, and are able to drive feeding across physiologic and behavioral contexts, including circadian cycles, social interaction, threat detection, and pain [36, 38, 72–75]. Here, we identify for the first time the time scale required for AgRP neurons to drive food intake during ABA, a condition of unique behavioral adaptations, including hyperactivity. Activation of AgRP neurons in this study was performed either during the initiation of the dark cycle, when mice typically begin eating, or in a period without food access (light cycle). As a previous report suggested, activation of AgRP neurons during the light cycle in ABA mice without food present promotes hyperactivity and fails to rescue bodyweight loss, clarifying the necessity of food availability for AgRP-mediated ABA reversal [44]. Indeed, AgRP neurons are inhibited following exercise in food-restricted states, suggesting that artificial activation of this population during restriction might drive behaviors intended to promote inhibition (e.g. hyperactivity) and alleviate the aversive nature of AgRP activation [43, 44, 59]. Furthermore, our studies indicate that artificial inhibition of AgRP neurons before food access in ABA worsens bodyweight loss at least partially due to enhanced hyperactivity. However, ABA bodyweight loss is also likely a result of activity-independent changes in energy expenditure, as chemogentic AgRP activation increases oxygen consumption. Together, these results propose that endogenous AgRP activity is carefully maintained to promote appropriate energy intake versus expenditure, and that the AgRP circuit is both necessary and sufficient for bodyweight maintenance in food restricted and ABA conditions.

A diversity of literature describes overall food intake in ABA, and yet no overarching consensus has been made on the microstructure of food intake during this condition. Here, we used specialized devices [49] to detect nuanced feeding bouts more accurately in mice. As a universal analysis criteria for the determination of meal patterns is lacking, we leveraged our control cohort (FR) to determine the mean interpellet interval (IPI) that occurs over the course of multiple days of food restriction, potentially identifying a new approach for future meal detection analyses. Using this criteria, we are able to highlight decreased meal number as a component of the decreased overall feeding observed during ABA. The peripheral and neural mechanisms underlying differences in meal size and meal number are largely unknown. While it is well documented that AGRP is elevated during hyperactive anorexia in humans and rodents, it is unclear if this elevation drives the altered meal patterns we observed [27–31]. Despite this elevation, we demonstrate that feeding-induced inhibition of AgRP neural activity is dysregulated during ABA. It is conceivable that these alterations in AgRP activity in response to food intake drive the observed behavioral abnormalities, but this has not yet been tested.

The ABA behavioral paradigm is a well-established rodent model of anorexia nervosa (AN) [21, 22], that allows for robust longitudinal recordings and manipulations of specific

cellular populations in a behaving individual that are not possible in many other species (i.e. humans). Indeed, we replicated previous studies indicating that rodents on the ABA paradigm phenocopy many of the behavioral maladaptations observed in human AN patients, including reduced food intake and hyperactivity. Yet, there are limitations of this model which warrant the careful consideration of our results in the overall context of AN. Most notably, ABA is an acute model of weight loss (not a chronic disease like AN) that is experimentally controlled. For example, individuals on the ABA paradigm do not have free access to food at all times, animals are socially isolated, and animals are genetically very similar (and sometimes genetically identical), all of which are (oftentimes) different conditions than patients experiencing AN. Additionally, while hyperactivity occurs in a large proportion of AN patients, not all AN patients display hyperactivity. Future studies are required to continue developing and updating rodent behavioral paradigms that can increase the implications of findings observed in rodent models of AN to the pathogenesis of the disease in humans.

Taken together, we have ascertained the unique capability, necessity and circadian timeframe required for AgRP neurons to ameliorate ABA despite disrupted neural activity responses to food. While these studies measure bulk activity responses to food intake, subsequent studies will be required to identify if AgRP neuronal activity dynamics are heterogenous using single-cell imaging techniques. Furthermore, future studies aimed at characterizing the molecular changes in AgRP neurons following ABA have the potential to elucidate the cellular mechanisms coordinating these changes, and thus greatly advance the collective understanding of feeding behavior during states of negative energy balance.

Supplementary Material

Refer to Web version on PubMed Central for supplementary material.

ACKNOWLEDGEMENTS

We would like to thank Dr. Alexxai Kravitz for the development of and extensive help with FED3 devices. We thank Dr. Bryan Roth for the CNO used in chemogenetic experiments. We also thank N. Martin and B. Gloss of the NIEHS Viral Vector Core for producing the AAVs used in chemogenetic experiments. We thank all members of Dr. Krashes' lab for technical support and guidance during this project. This research was supported by the Intramural Research Program of the National Institutes of Health, the National Institutes of Diabetes and Digestive and Kidney Diseases (DK075088 to M.J.K. and DK075087-06 to M.J.K.) and the Nancy Nossal Fellowship (NIH-NIDDK; to A.K.S.-H.).

REFERENCES

1. Diagnostic and statistical manual of mental disorders: DSM-5™, 5th ed. 2013;5:5.
2. Kaye WH, Wierenga CE, Bailer UF, Simmons AN, Bischoff-Grethe A. Nothing tastes as good as skinny feels: the neurobiology of anorexia nervosa. Trends Neurosci. 2013;36:110–20. [PubMed: 23333342]
3. Spring VL, Bulik CM. Implicit and explicit affect toward food and weight stimuli in anorexia nervosa. Eat Behav. 2014;15:91–94. [PubMed: 24411758]
4. Kaye W Neurobiology of anorexia and bulimia nervosa. Physiol Behav. 2008;94:121–35. [PubMed: 18164737]
5. Holsen LM, Lawson EA, Blum J, Ko E, Makris N, Fazeli PK, et al. Food motivation circuitry hypoactivation related to hedonic and nonhedonic aspects of hunger and satiety in women with

active anorexia nervosa and weight-restored women with anorexia nervosa. J Psychiatry Neurosci. 2012;37:322–32. [PubMed: 22498079]

6. Stern SA, Bulik CM Alternative Frameworks for Advancing the Study of Eating Disorders. Trends Neurosci. 30 October 2020. 10.1016/j.tins.2020.10.001.
7. Wonderlich SA, Bulik CM, Schmidt U, Steiger H, Hoek HW. Severe and enduring anorexia nervosa: Update and observations about the current clinical reality. Int J Eat Disord. 2020;53:1303–12. [PubMed: 32359125]
8. Clausen L, Jones A. A systematic review of the frequency, duration, type and effect of involuntary treatment for people with anorexia nervosa, and an analysis of patient characteristics. J Eat Disord. 2014;2:29. [PubMed: 25414793]
9. Bargiacchi A, Clarke J, Paulsen A, Leger J. Refeeding in anorexia nervosa. Eur J Pediatr. 2019;178:413–22. [PubMed: 30483963]
10. Mitchell JE, Peterson CB. Anorexia Nervosa. N. Engl J Med. 2020;382:1343–51. [PubMed: 32242359]
11. Fichter MM, Quadflieg N. Mortality in eating disorders - results of a large prospective clinical longitudinal study. Int J Eat Disord. 2016;49:391–401. [PubMed: 26767344]
12. Hardaway JA, Crowley NA, Bulik CM, Kash TL. Integrated circuits and molecular components for stress and feeding: implications for eating disorders. Genes Brain Behav. 2015;14:85–97. [PubMed: 25366309]
13. Wu J, Liu J, Li S, Ma H, Wang Y. Trends in the prevalence and disability-adjusted life years of eating disorders from 1990 to 2017: results from the Global Burden of Disease Study 2017. Epidemiol Psychiatr. Science 2020;29:e191.
14. Massa MG, Correa SM. Sexes on the brain: Sex as multiple biological variables in the neuronal control of feeding. Biochim Biophys Acta Mol Basis Dis. 2020;1866:165840. [PubMed: 32428559]
15. Kron L, Katz JL, Gorzynski G, Weiner H. Hyperactivity in anorexia nervosa: a fundamental clinical feature. Compr Psychiatry. 1978;19:433–40. [PubMed: 679677]
16. Achamrah N, Coëffier M, Déchelotte P. Physical activity in patients with anorexia nervosa. Nutr Rev. 2016;74:301–11. [PubMed: 27052638]
17. Harris A, Hay P, Touyz S. Psychometric properties of instruments assessing exercise in patients with eating disorders: a systematic review. J Eat Disord. 2020;8:45. [PubMed: 32884810]
18. Gorrell S, Flatt RE, Bulik CM, Le Grange D Psychosocial etiology of maladaptive exercise and its role in eating disorders: A systematic review. Int J Eat Disord. 4 May 2021. 10.1002/eat.23524.
19. Pirke KM, Broocks A, Wilckens T, Marquard R, Schweiger U. Starvation-induced hyperactivity in the rat: the role of endocrine and neurotransmitter changes. Neurosci Biobehav Rev. 1993;17:287–94. [PubMed: 7903806]
20. Routtenberg A, Kuznesof AW. Self-starvation of rats living in activity wheels on a restricted feeding schedule. J Comp Physiol Psychol. 1967;64:414–21. [PubMed: 6082873]
21. Gutierrez E. A rat in the labyrinth of anorexia nervosa: contributions of the activity-based anorexia rodent model to the understanding of anorexia nervosa. Int J Eat Disord. 2013;46:289–301. [PubMed: 23354987]
22. Schalla MA, Stengel A. Activity Based Anorexia as an Animal Model for Anorexia Nervosa-A Systematic Review. Front Nutr. 2019;6:69. [PubMed: 31165073]
23. Guisinger S. Adapted to flee famine: adding an evolutionary perspective on anorexia nervosa. Psychol Rev. 2003;110:745–61. [PubMed: 14599241]
24. Foldi CJ, Milton LK, Oldfield BJ. A focus on reward in anorexia nervosa through the lens of the activity-based anorexia rodent model. J Neuroendocrinol. 2017;29.
25. Vink T, Hinney A, van Elburg AA, van Goozen SH, Sandkuijl LA, Sinke RJ, et al. Association between an agouti-related protein gene polymorphism and anorexia nervosa. Mol Psychiatry. 2001;6:325–8. [PubMed: 11326303]
26. Dardennes RM, Zizzari P, Tolle V, Foulon C, Kipman A, Romo L, et al. Family trios analysis of common polymorphisms in the obestatin/ghrelin, BDNF and AGRP genes in patients with Anorexia nervosa: association with subtype, body-mass index, severity and age of onset. Psychoneuroendocrinology. 2007;32:106–13. [PubMed: 17197106]

27. Moriya J, Takimoto Y, Yoshiuchi K, Shimosawa T, Akabayashi A. Plasma agouti-related protein levels in women with anorexia nervosa. Psychoneuroendocrinology. 2006;31:1057–61. [PubMed: 16904835]
28. Merle JV, Haas V, Burghardt R, Döhler N, Schneider N, Lehmkuhl U, et al. Agouti-related protein in patients with acute and weight-restored anorexia nervosa. Psychol Med. 2011;41:2183–92. [PubMed: 21426605]
29. de Rijke CE, Hillebrand JJG, Verhagen LAW, Roeling TAP, Adan RAH. Hypothalamic neuropeptide expression following chronic food restriction in sedentary and wheel-running rats. J Mol Endocrinol. 2005;35:381–90. [PubMed: 16216917]
30. Kas MJH, van Dijk G, Scheurink AJW, Adan RAH. Agouti-related protein prevents self-starvation. Mol Psychiatry. 2003;8:235–40. [PubMed: 12610657]
31. Rokot NT, Ataka K, Iwai H, Suzuki H, Tachibe H, Kairupan TS, et al. Antagonism for NPY signaling reverses cognitive behavior defects induced by activity-based anorexia in mice. Psychoneuroendocrinology. 2021;126:105133. [PubMed: 33540372]
32. Hillebrand JJG, Kas MJH, Scheurink AJW, van Dijk G, Adan RAH. AgRP(83-132) and SHU9119 differently affect activity-based anorexia. Eur Neuropsychopharmacol. 2006;16:403–12. [PubMed: 16360312]
33. Krashes MJ, Koda S, Ye C, Rogan SC, Adams AC, Cusher DS, et al. Rapid, reversible activation of AgRP neurons drives feeding behavior in mice. J Clin Invest. 2011;121:1424–8. [PubMed: 21364278]
34. Aponte Y, Atasoy D, Sternson SM. AGRP neurons are sufficient to orchestrate feeding behavior rapidly and without training. Nat Neurosci. 2011;14:351–5. [PubMed: 21209617]
35. Chen Y, Lin Y-C, Zimmerman CA, Essner RA, Knight ZA. Hunger neurons drive feeding through a sustained, positive reinforcement signal. Elife. 2016;5:e18640. [PubMed: 27554486]
36. Essner RA, Smith AG, Jamnik AA, Ryba AR, Trutner ZD, Carter ME. AgRP Neurons Can Increase Food Intake during Conditions of Appetite Suppression and Inhibit Anorexigenic Parabrachial Neurons. J Neurosci. 2017;37:8678–87. [PubMed: 28821663]
37. Burnett CJ, Li C, Webber E, Tsaousidou E, Xue SY, Brüning JC, et al. Hunger-Driven Motivational State Competition. Neuron. 2016;92:187–201. [PubMed: 27693254]
38. Burnett CJ, Funderburk SC, Navarrete J, Sabol A, Liang-Guallpa J, Desrochers TM, et al. Need-based prioritization of behavior. Elife. 2019;8:e44527. [PubMed: 30907726]
39. Chen Y, Lin Y-C, Kuo T-W, Knight ZA. Sensory Detection of Food Rapidly Modulates Arcuate Feeding Circuits. Cell. 2015;160:829–41. [PubMed: 25703096]
40. Beutler LR, Chen Y, Ahn JS, Lin Y-C, Essner RA, Knight ZA. Dynamics of Gut-Brain Communication Underlying Hunger. Neuron. 2017;96:461–475.e5. [PubMed: 29024666]
41. Su Z, Alhadeff AL, Betley JN. Nutritive, Post-ingestive Signals Are the Primary Regulators of AgRP Neuron Activity. Cell Rep. 2017;21:2724–36. [PubMed: 29212021]
42. Betley JN, Xu S, Cao ZFH, Gong R, Magnus CJ, Yu Y, et al. Neurons for hunger and thirst transmit a negative-valence teaching signal. Nature. 2015;521:180–5. [PubMed: 25915020]
43. He Z, Gao Y, Alhadeff AL, Castorena CM, Huang Y, Lieu L, et al. Cellular and synaptic reorganization of arcuate NPY/AgRP and POMC neurons after exercise. Mol Metab. 2018;18:107–19. [PubMed: 30292523]
44. Miletta MC, Iyilikci O, Shanabrough M, Šestan-Peša M, Cammisa A, Zeiss CJ, et al. AgRP neurons control compulsive exercise and survival in an activity-based anorexia model. Nat Metab. 2020;2:1204–11. [PubMed: 33106687]
45. Beeler JA, Mourra D, Zanca RM, Kalmbach A, Gellman C, Klein BY, et al. Vulnerable and Resilient Phenotypes in a Mouse Model of Anorexia Nervosa. Biol Psychiatry. 16 July 2020. 10.1016/j.biopsych.2020.06.030.
46. Milton LK, Oldfield BJ, Foldi CJ. Evaluating anhedonia in the activity-based anorexia (ABA) rat model. Physiol Behav. 2018;194:324–32. [PubMed: 29913226]
47. Milton LK, Patton T, O'Keeffe M, Oldfield BJ, Foldi CJ. In pursuit of biomarkers for predicting susceptibility to activity-based anorexia in adolescent female rats. Int J Eat Disord. 2022;55:664–77. [PubMed: 35302253]

48. Hurley MM, Murlanova K, Macias LK, Sabir AI, O'Brien SC, Bhasin H, et al. Activity-based anorexia disrupts systemic oxidative state and induces cortical mitochondrial fission in adolescent female rats. Int J Eat Disord. 2021;54:639–45. [PubMed: 33368559]
49. Matikainen-Ankney BA, Earnest T, Ali M, Casey E, Wang JG, Sutton AK, et al. An open-source device for measuring food intake and operant behavior in rodent home-cages. Elife. 2021;10.
50. Foldi CJ, Milton LK, Oldfield BJ. The Role of Mesolimbic Reward Neurocircuitry in Prevention and Rescue of the Activity-Based Anorexia (ABA) Phenotype in Rats. Neuropsychopharmacology. 2017;42:2292–2300. [PubMed: 28322236]
51. Milton LK, Mirabella PN, Greaves E, Spanswick DC, van den Buuse M, Oldfield BJ, et al. Suppression of Corticostriatal Circuit Activity Improves Cognitive Flexibility and Prevents Body Weight Loss in Activity-Based Anorexia in Rats. Biol Psychiatry. 2 July 2020. 10.1016/j.biopsych.2020.06.022.
52. Verhagen LAW, Luijendijk MCM, Hillebrand JJG, Adan RAH. Food-anticipatory activity in activity-based anorexia: The involvement of dopamine. Appetite. 2007;49:337.
53. Daimon CM, Hentges ST. β-endorphin differentially contributes to food anticipatory activity in male and female mice undergoing activity-based anorexia. Physiol Rep. 2021;9:e14788. [PubMed: 33661571]
54. Daimon CM, Hentges ST. Inhibition of POMC neurons in mice undergoing activity-based anorexia selectively blunts food anticipatory activity without affecting body weight or food intake. Am J Physiol Regul Integr Comp Physiol. 2022;322:R219–R227. [PubMed: 35043681]
55. Scharner S, Prinz P, Goebel-Stengel M, Kobelt P, Hofmann T, Rose M, et al. Activity-Based Anorexia Reduces Body Weight without Inducing a Separate Food Intake Microstructure or Activity Phenotype in Female Rats-Mediation via an Activation of Distinct Brain Nuclei. Front Neurosci. 2016;10:475. [PubMed: 27826222]
56. Schwartz GJ, Zeltser LM. Functional organization of neuronal and humoral signals regulating feeding behavior. Annu Rev Nutr. 2013;33:1–21. [PubMed: 23642202]
57. Azevedo EP, Ivan VJ, Friedman JM, Stern SA. Higher-Order Inputs Involved in Appetite Control. Biol Psychiatry. 2022;91:869–78. [PubMed: 34593204]
58. Mandelblat-Cerf Y, Ramesh RN, Burgess CR, Patella P, Yang Z, Lowell BB, et al. Arcuate hypothalamic AgRP and putative POMC neurons show opposite changes in spiking across multiple timescales. Elife. 2015;4:e07122. [PubMed: 26159614]
59. Dietrich MO, Zimmer MR, Bober J, Horvath TL. Hypothalamic Agrp Neurons Drive Stereotypic Behaviors beyond Feeding. Cell. 2015;160:1222–32. [PubMed: 25748653]
60. Padilla SL, Qiu J, Soden ME, Sanz E, Nestor CC, Barker FD, et al. Agouti-related peptide neural circuits mediate adaptive behaviors in the starved state. Nat Neurosci. 2016;19:734–41. [PubMed: 27019015]
61. Betley JN, Cao ZFH, Ritola KD, Sternson SM. Parallel, redundant circuit organization for homeostatic control of feeding behavior. Cell. 2013;155:1337–50. [PubMed: 24315102]
62. Alexander GM, Rogan SC, Abbas AI, Armbruster BN, Pei Y, Allen JA, et al. Remote Control of Neuronal Activity in Transgenic Mice Expressing Evolved G Protein-Coupled Receptors. Neuron. 2009;63:27–39. [PubMed: 19607790]
63. Zhu H, Aryal DK, Olsen RHJ, Urban DJ, Swearingen A, Forbes S, et al. Cre-dependent DREADD (Designer Receptors Exclusively Activated by Designer Drugs) mice. Genesis. 2016;54:439–46. [PubMed: 27194399]
64. Klenotich SJ, Ho EV, McMurray MS, Server CH, Dulawa SC. Dopamine D2/3 receptor antagonism reduces activity-based anorexia. Transl Psychiatry. 2015;5:e613. [PubMed: 26241351]
65. Welch AC, Zhang J, Lyu J, McMurray MS, Javitch JA, Kellendonk C, et al. Dopamine D2 receptor overexpression in the nucleus accumbens core induces robust weight loss during scheduled fasting selectively in female mice. Mol Psychiatry. 2021;26:3765–77. [PubMed: 31863019]
66. Beutler LR, Corpuz TV, Ahn JS, Kosar S, Song W, Chen Y, et al. Obesity causes selective and long-lasting desensitization of AgRP neurons to dietary fat. Elife. 2020;9:e55909. [PubMed: 32720646]

67. Mazzone CM, Liang-Guallpa J, Li C, Wolcott NS, Boone MH, Southern M, et al. High-fat food biases hypothalamic and mesolimbic expression of consummatory drives. Nat Neurosci. 2020;23:1253–66. [PubMed: 32747789]

68. Lippert RN, Hess S, Klemm P, Burgeno LM, Jahans-Price T, Walton ME, et al. Maternal high-fat diet during lactation reprograms the dopaminergic circuitry in mice. J Clin Invest. 2020;130:3761–76. [PubMed: 32510473]

69. Lippert RN, Brüning JC. Maternal Metabolic Programming of the Developing Central Nervous System: Unified Pathways to Metabolic and Psychiatric Disorders. Biol Psychiatry. 2022;91:898–906. [PubMed: 34330407]

70. Cai X, Liu H, Feng B, Yu M, He Y, Liu H, et al. A D2 to D1 shift in dopaminergic inputs to midbrain 5-HT neurons causes anorexia in mice. Nat Neurosci. 2022;25:646–58. [PubMed: 35501380]

71. Lockie SH, Stark R, Mequinion M, Ch'ng S, Kong D, Spanswick DC, et al. Glucose Availability Predicts the Feeding Response to Ghrelin in Male Mice, an Effect Dependent on AMPK in AgRP Neurons. Endocrinology. 2018;159:3605–14. [PubMed: 30204871]

72. Gropp E, Shanabrough M, Borok E, Xu AW, Janoschek R, Buch T, et al. Agouti-related peptide–expressing neurons are mandatory for feeding. Nat Neurosci. 2005;8:1289–91. [PubMed: 16158063]

73. Luquet S, Perez FA, Hnasko TS, Palmiter RD. NPY/AgRP Neurons Are Essential for Feeding in Adult Mice but Can Be Ablated in Neonates. Science. 2005;310:683–5. [PubMed: 16254186]

74. Goldstein N, Levine BJ, Loy KA, Duke WL, Meyerson OS, Jamnik AA, et al. Hypothalamic Neurons that Regulate Feeding Can Influence Sleep/Wake States Based on Homeostatic Need. Curr Biol. 2018;28:3736–47. [PubMed: 30471995]

75. Alhadeff AL, Su Z, Hernandez E, Klima ML, Phillips SZ, Holland RA, et al. A Neural Circuit for the Suppression of Pain by a Competing Need State. Cell. 2018;173:140–152.e15. [PubMed: 29570993]

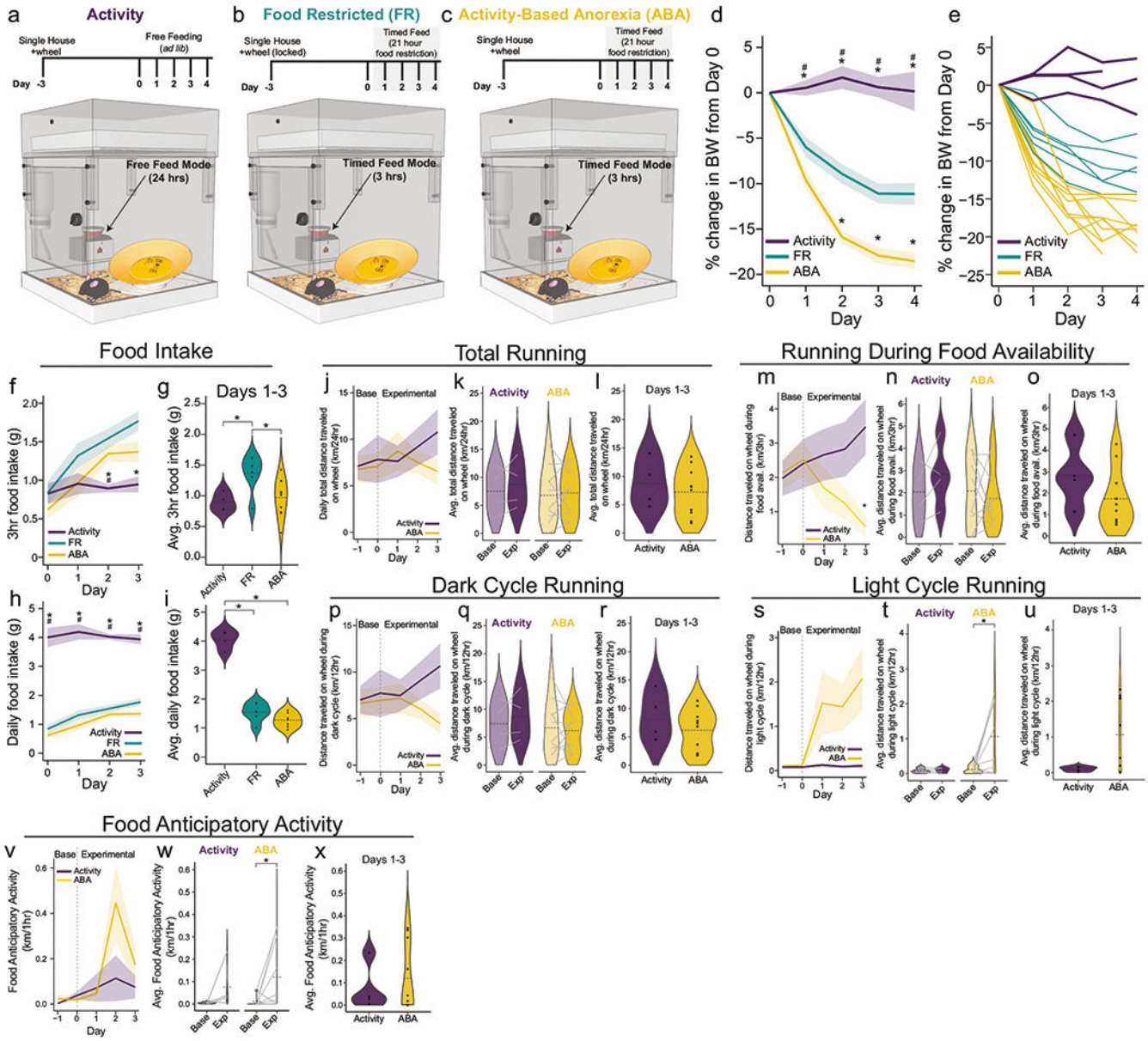

Fig. 1. Food restriction with voluntary running wheel access causes activity-based anorexia.

a–c Schematic of experimental set-up, in which mice are trained on a wireless voluntary running wheel in their homecage (Activity, Activity-Based Anorexia, ABA) or a locked running wheel (Food Restricted, FR,). Following wheel habituation, ABA and FR mice begin a 21 h food restriction paradigm, in which food is available the first three hours of the dark cycle (beginning after the first three hours of the dark cycle on Day 0). **d, e** ABA mice lose more bodyweight than FR mice (Day 2–4 $p < 0.01$), whereas bodyweight of Activity mice remains constant. **f** In ad libitum fed conditions (Day 0), ABA, Activity and FR mice eat similarly ($p > 0.65$), whereas food restriction in ABA and FR mice (Days 1–3) causes mice to eat more than Activity mice in the 3 h period of food availability over the course of the paradigm (p values from Days 1–3 in order: Activity vs. FR $p = 0.378$ (n.s.), $p = 0.008$, $p = 0.006$; Activity vs. ABA $p = 1$ (n.s.), $p = 0.012$, $p = 0.121$ (n.s.)). **g** FR

mice consume more averaged food during food availability over the course of days with food restriction (Days 1–3) than both ad libitum fed Activity mice ($p = 0.049$), as well as similarly food restricted ABA mice ($p = 0.038$). **h** Ad libitum fed Activity mice eat more than both ABA and FR cohorts over the entire 24 h period (Activity vs. ABA/FR Days 0–3 $p < 0.01$), and when averaged across food restriction days (**i**, Activity vs. ABA/FR $p < 0.0001$). **j–l** ABA mice display no difference than ad libitum fed Activity controls in total voluntary running when measured over the course of the experiment (including a baseline day (Day −1) when mice were not yet food restricted, $p = 0.67$), when comparing average distance traveled on the wheel during baseline (Day −1) vs. experimental (Days 0-3) (baseline vs. experimental: Activity $p = 0.41$, ABA $p = 0.74$), or just during the experimental days ($p = 0.55$). **m–o** Following food restriction in ABA mice, running during food availability decreases compared to ad libitum fed Activity mice, but is not significantly different until Day 3 of food restriction ($p = 0.03$). Yet, when averaged across days of restriction, neither ABA nor Activity mice show decreased running during the first three hours of the dark cycle (when food is available for ABA mice) compared to baseline days (baseline vs. experimental: Activity $p = 0.27$, ABA $p = 0.59$). Similarly, ABA mice do not show decreased wheel running compared to Activity mice during food availability averaged across experimental days ($p = 0.21$). **p–r** Wheel running during the active dark cycle is not changed in ABA mice compared to Activity mice when measured daily ($p = 0.086$), when compared between baseline and experimental days (baseline vs. experimental: Activity $p = 0.416$, ABA $p = 0.709$), or when averaged across experimental days only ($p = 0.287$). **s–u** While Activity mice run minimally on the running wheel during the light cycle throughout the experiment, ABA mice increase wheel running during the light cycle upon food restriction compared to baseline (baseline vs. experimental: Activity $p = 0.493$, ABA $p = 0.016$). **v–x** Food anticipatory activity (FAA; measured by total voluntary wheel running one hour prior to the onset of food availability/dark cycle onset) was elevated in ABA mice upon food restriction compared to baseline levels, whereas FAA in Activity mice is unchanged (w, baseline vs. experimental: Activity $p = 0.274$, ABA $p = 0.047$). Wheel: $n =$ 3-4, FR: $n = 6$, ABA: $n = 8–10$. Significance determined by $p < 0.05$ using a two-way mixed ANOVA followed by Bonferroni post-hoc if appropriate (**d**, **f**, **h**, **j**, **m**, **p**, **s**), a one-way ANOVA followed by Tukey post-hoc if appropriate (**g**, **i**), a paired ***t***-test (**k**, **n**, **q**, **t**), or an unpaired ***t***-test (**l**, **o**, **r**, **u**). Data are represented as mean ± SEM (**d–f**, **h**, **j**, **m**, **p**, **s**), or as a violin plot with dotted lines at the mean (**g**, **i**, **k**, **l**, **n**, **o**, **q**, **r**, **t**, **u**).

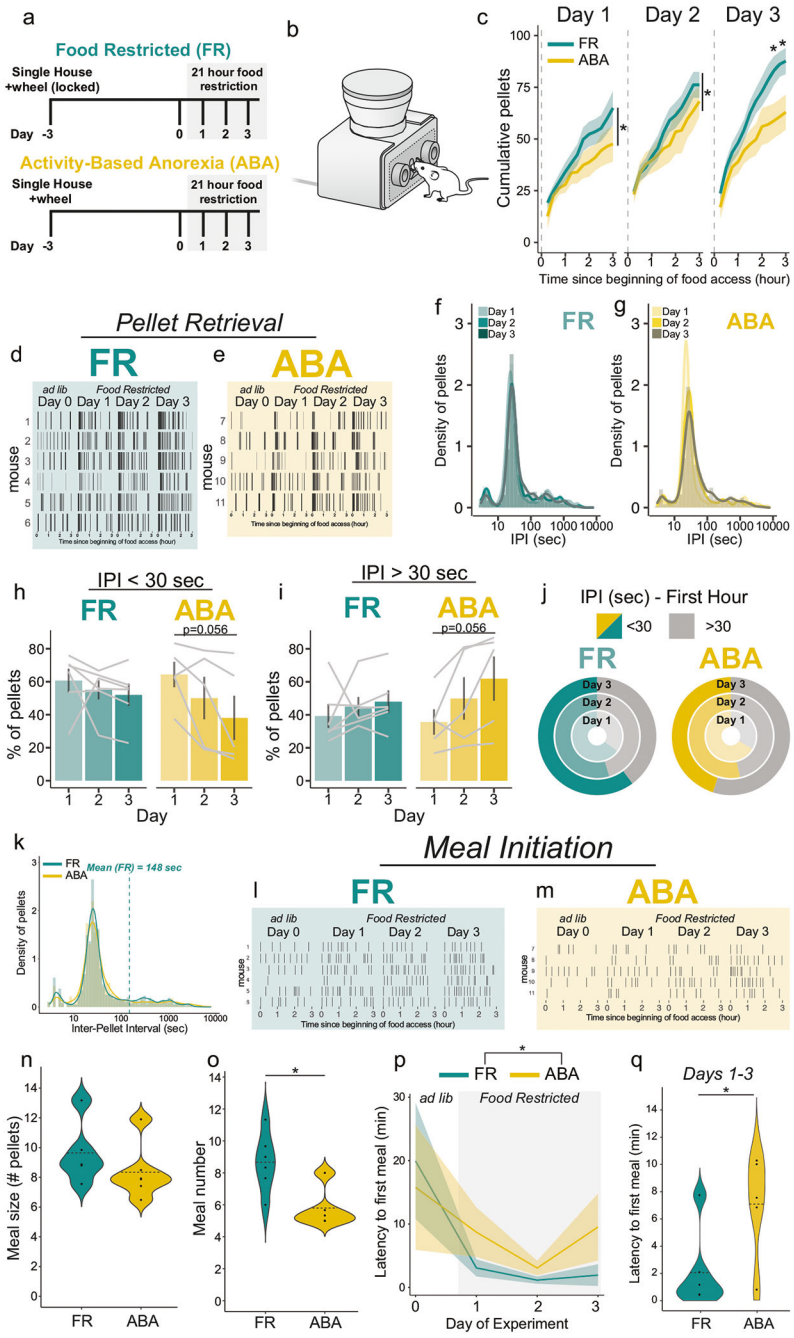

Fig. 2. ABA mice demonstrate decreased food intake due to diminished meal number.

a, **b** Precise measurements of 3 h feeding behavior were performed in FR and ABA mice using the Feeding Experimental Device (FED3), throughout the paradigm. **c** Cumulative pellet intake over the course of feeding indicates ABA mice eat less than FR mice on all days of food restriction (Day 1: $p = 0.05$, Day 2: $p = 0.015$, Day 3: $p < 0.0001$). **d**, **e** Raster plots of individual pellet retrieval from FEDs reveals potential inter-pellet interval and corresponding meal pattern differences in FR (left) and ABA (right) mice. **f**, **g** Kernel density estimation (KDE) curves indicate that FR mice maintain similar IPI frequencies

throughout multiple days of food restriction, whereas the KDE curve of IPI in ABA mice shifts right after the first day of food deprivation. **h**, **i** The percentage of pellets eaten with an interpellet interval (IPI) < 30 s (h) or IPI ≥ 30 s is unaltered for FR mice across days of the paradigm, whereas ABA mice show trends towards decreased and increased frequency of pellets eaten with these IPIs, respectively ($p = 0.056$). **j** Binned pellets from all mice within FR or ABA cohorts further exhibit progressively greater retrieval times in ABA mice (yellow/gray, right), compared to FR mice (green/gray, left). **k** KDE plot of IPI across all days of food restriction (Days 1-3) demonstrates that the mean IPI in FR mice is 148.2 s, which was subsequently used for meal pattern detection in all mice (i.e. 2+ pellets consumed within 148.2 sof each other). **l, m** Raster plots of meal bout initiation timepoints highlights that ABA mice demonstrate a potential decrease in the number of meals initiated over on food restricted days (Days 1-3) when compared to FR mice. While meal size is comparable between FR and ABA mice (**n**), meal number is decreased in mice on the ABA paradigm compared to FR mice (**o**; $p = 0.016$). **p**, **q** The latency to the first meal is altered in ABA mice in comparison to FR mice, when observed across the experimental paradigm (p, main effect of experimental condition, $p = 0.033$) or when averaged across food restriction days (q, $p = 0.044$). Significance determined by $p < 0.05$ using a two-way ANOVA followed by Bonferroni post-hoc if appropriate (**c**, **h**, **i**, **p**), or an unpaired t-test (**n**, **o**, **q**). FR $n = 6$; ABA $n = 5$. Data represented as mean ± SEM (**c**, **h**, **i**, **p**), or as a violin plot with dotted lines at the mean (**n**, **o**, **q**).

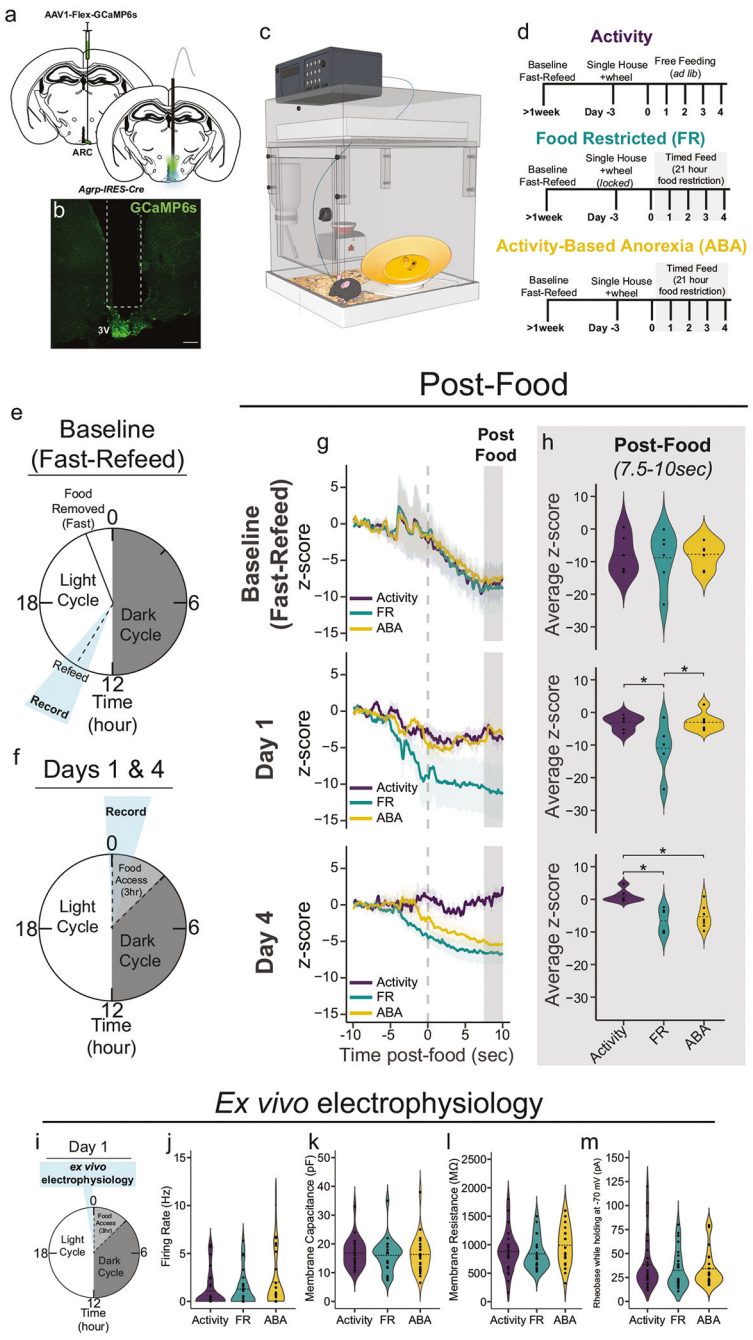

Fig. 3. AgRP neuronal inhibition following food intake is dysregulated in ABA mice.

a, **b** Agrp-ires-Cre mice were injected with AAV1-hSyn-Flex-GCaMP6s and a fiber placed above the ARC to record AgRP calcium signaling in freely-moving photometry experiments. **c** Behavioral set-up, in which mice are housed in phenotyper cages containing FEDs and voluntary running wheels, with AgRP calcium activity monitoring via fiber photometry patch cords that allow for free movement. **d** Mice were placed in three different behavioral cohorts to measure AgRP activity in response to food intake in mice that engage in voluntary exercise absent food restriction (Activity), restricted feeding without running

(FR), or voluntary running in addition to food restriction (ABA). **e** At least one week before experiments began, AgRP activity was measured in response to a fast-refeed across all mice. **f** On Day 1 and Day 4 of the paradigm, mice were hooked up to the fiber patchcord at least 1 h before experiments began, and recordings began prior to food availability (**f**, blue). **g**, **h**, top panel AgRP neuronal inhibition is similar across all behavioral groups in response to food presentation ($t = 0$) in the fasted condition before being placed in experimental cohorts. **g**, **h**, middle panel On Day 1, food retrieval significantly decreases AgRP population activity in FR mice compared to ad libitum fed Activity controls (averaged across t = 7.5-10 sec of Post-Pellet (grey), Activity vs. FR $p = 0.038$), whereas this decrease is not observed in ABA mice (ABA vs. Activity $p = 0.996$; ABA vs. FR $p = 0.027$). **g**, **h**, bottom panel By Day 4 of food restriction, AgRP activity remains decreased in response to food retrieval in FR mice compared to Activity controls (Activity vs. FR $p = 0.002$). The diminished AgRP inhibition observed on Day 1 of food restriction in ABA mice is no longer observed on Day 4, and thus ABA mice more closely resemble FR mice than ad libitum fed Activity mice (ABA vs. Activity $p = 0.007$, ABA vs. FR $p = 0.761$). **i–m** Ex vivo electrophysiology experiments were performed in AgRP neurons from NPY-hrGFP or AgRP-iCre,ZsGreen reporter mice on Day 1 of the paradigm across conditions immediately prior to the onset of the dark cycle. Basal activity measurements were unchanged across Activity, FR, and ABA mice, including measurements of (**j**) firing rate, **k** membrane capacitance, **l** membrane resistance, or (**m**) rheobase while holding at −70 mV. Significance was determined by $p < 0.05$ using a one-way ANOVA followed by Tukey post-hoc if necessary (**h**, **k–m**). Photometry: Activity $n = 6$, FR $n = 5$-6; ABA $n = 7$; ex vivo electrophysiology: Activity $n = 4$ (27 cells), FR $n = 4$ (firing rate: 25 cells; all other measures: 24 cells), ABA $n = 5$ (27 cells). Data represented as mean ± SEM (**g**) or as a violin plot with dotted lines at the mean (**h**, **k–m**); scale bar = 200 μm.

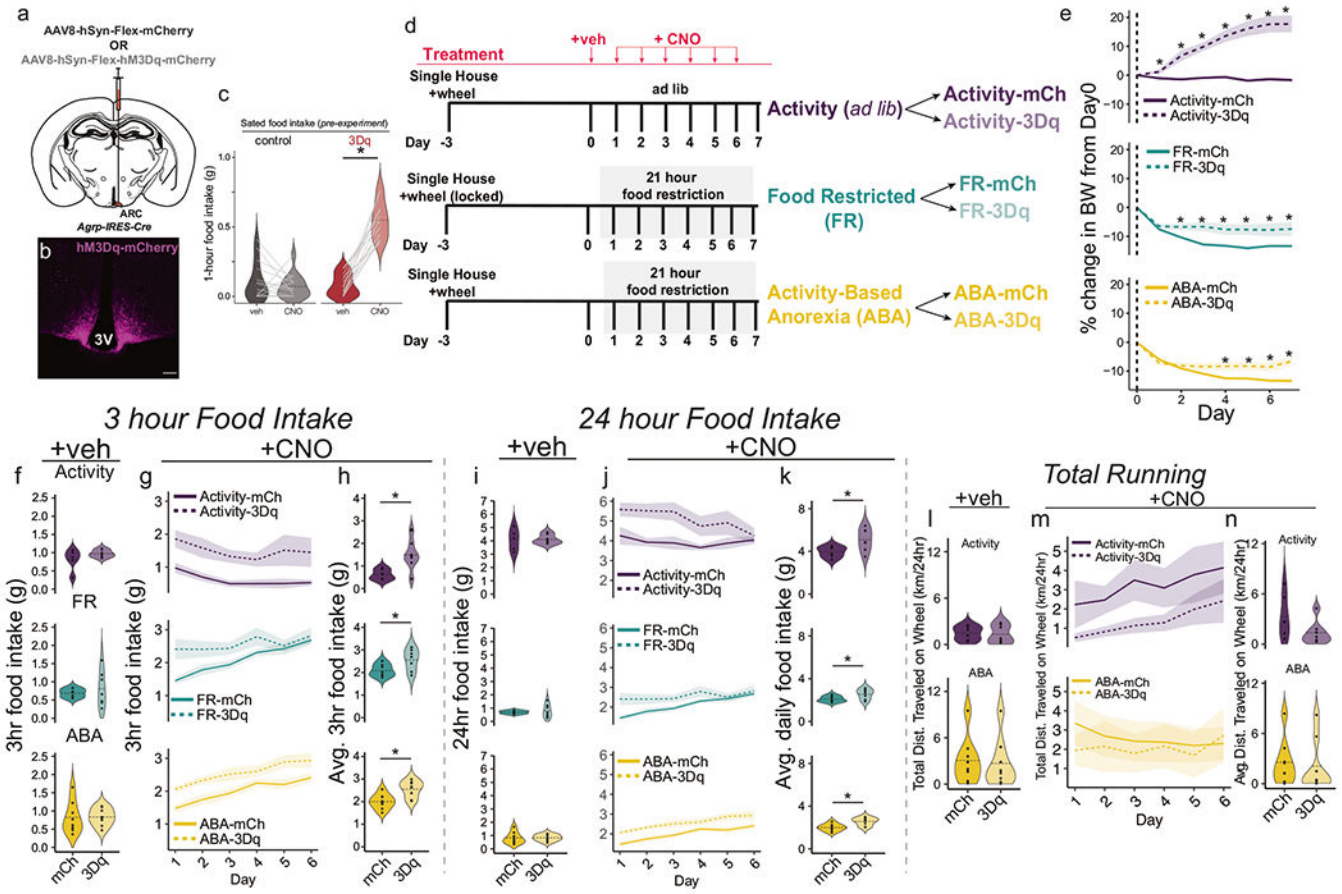

Fig. 4. AgRP activation ameliorates ABA development.

a AgRP neurons were artificially activated in AgRP-iCre mice via expression of 3Dq (using injection of AAV8-hSyn-Flex-hM3Dq-mCherry; 3Dq) and compared to control mice injected with AAV8-hSyn-Flex-mCherry (mCh). **b** Representative image of mCherry expression in the ARC of AgRP-iCre mice injected with AAV8-hSyn-Flex-hM3Dq-mCherry. **c** Validation of viral hits demonstrates that CNO injection in control mice does not alter food intake at the beginning of the inactive light period (black, veh vs CNO: $p = 0.373$), whereas 3Dq expression in AgRP neurons increases sated feeding (red, veh vs. CNO: $p < 0.0001$). **d** Outline of experiment, in which three behavioral groups each had control (Activity-mCh, FR-mCh, ABA-mCh) and experimental groups (Activity-3Dq, FR-3Dq, ABA-3Dq). All mice were injected with vehicle on Day 0 of the paradigm. Following 3 h of feeding at the onset of the dark cycle on Day 0, FR and ABA groups were food restricted, whereas Activity mice were continued on ad libitum feeding. On Days 1–6, all mice received injections of CNO (i.p., 1.0 mg/kg) 15 min prior to the onset of the dark cycle. **e** 3Dq-mediated AgRP activation (dashed lines) increases BW compared to mCh controls (solid lines) in Activity (top, purple; Day 2: $p = 0.003$, Days 3–7: $p < 0.001$), FR (middle, green; Day 2: $p = 0.021$, Day 3: $p = 0.007$, Day 4: $p = 0.024$, Day 5: $p = 0.011$, Day 6: $p = 0.049$, Day 7: $p = 0.049$) and ABA (bottom, yellow; Day 4: $p = 0.033$, Day 5: $p = 0.015$, Day 6: $p = 0.018$, Day 7: $p = 0.005$) mice. **f** 3 h and **i** 24 h food intake is comparable between mCh and 3Dq cohorts in response to vehicle injections on Day 0

(Activity (3 h): $p = 0.288$, FR (3 h & 24 h): $p = 0.548$, ABA (3 h & 24 h): $p = 0.939$, Activity (24 h): $p = 0.942$). 3Dq-mediated AgRP activation increases **g**, **h** 3 h and **j**, **k** 24 h feeding in Activity, FR and ABA 3Dq mice compared to mCh controls (averaged across CNO days (Days 1–6): Activity **h** $p = 0.013$, **k** $p = 0.032$; FR (**h** & **i**): $p = 0.0497$; ABA (**h** & **i**): $p = 0.006$). **l** Total voluntary running activity is comparable between mCh and 3Dq cohorts in response to vehicle injections on Day 0 (Activity $p = 0.839$, ABA $p = 0.802$). **m**, **n** 3Dq-mediated AgRP activation in Activity or ABA mice does not significantly change total voluntary running when measured over the course of CNO-injected days (Activity (top): $p = 0.0749$), ABA (bottom): $p = 0.132$). Significance determined by $p < 0.05$ using a paired *t*-test (**c**), a two-way ANOVA followed by Bonferroni post-hoc if appropriate (**e**, **g**, **j**, **m**) or an unpaired *t*-test (**f**, **h**, **i**, **k**, **l**, **n**). Activity-mCh $n = 5$-6; Activity-3Dq $n = 7$; FR-mCh $n = 7$; FR-3Dq $n = 7$; ABA-mCh $n = 8$; ABA-3 Dq $n = 8$. Data represented as mean ± SEM. (**e**, **g**, **j**, **m**), or as a violin plot with dotted lines at the mean (**c**, **f**, **h**, **i**, **k**, **l**, **n**).

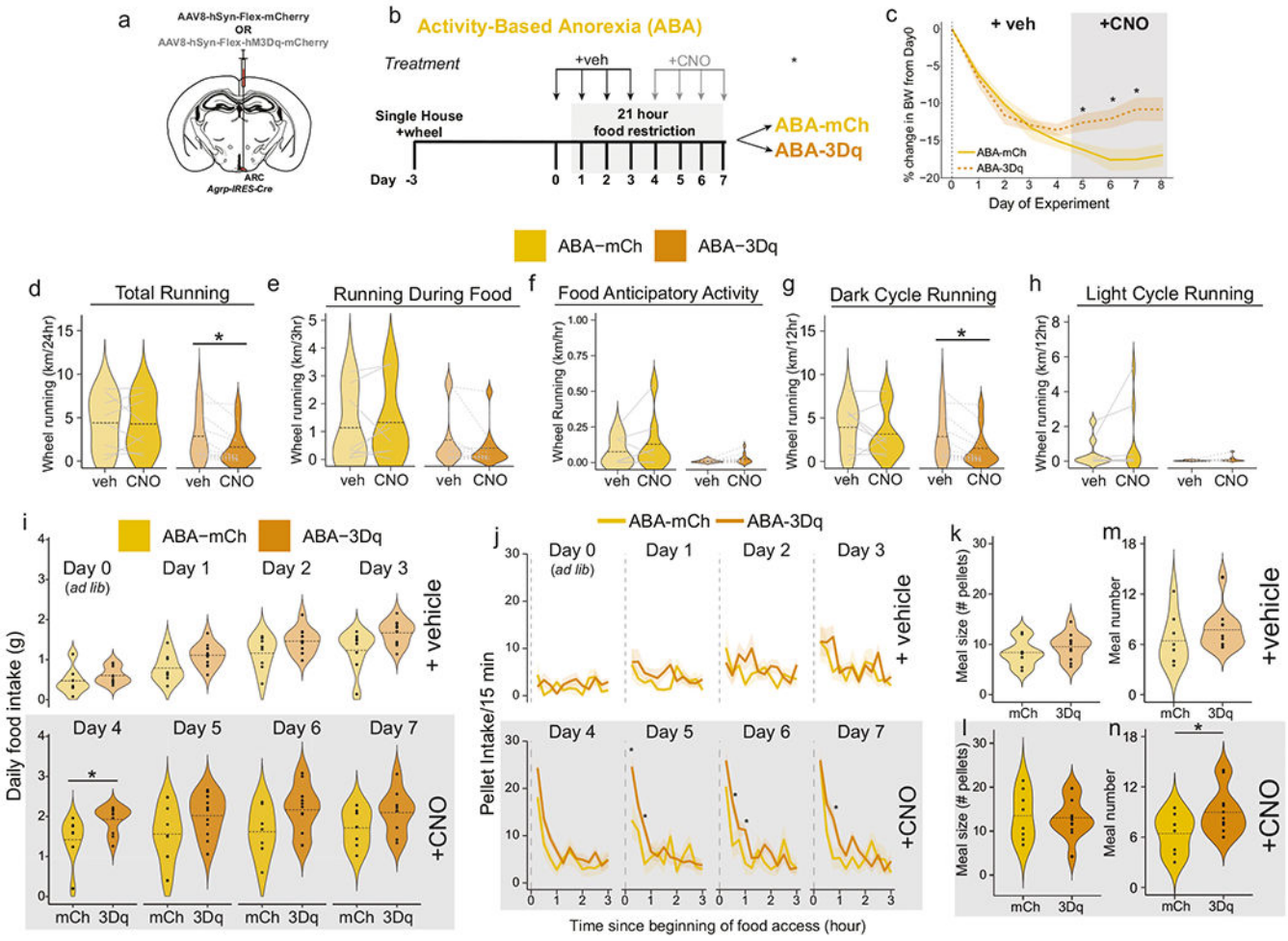

Fig. 5. ABA progression is rectified by AgRP activation during food availability after initial bodyweight loss.

a AgRP neurons were artificially activated in AgRP-iCre mice via expression of 3 Dq (using injection of AAV8-hSyn-Flex-hM3Dq-mCherry; 3Dq) and compared to control mice injected with AAV8-hSyn-Flex-mCherry (mCh). **b** ABA paradigm where mice were injected with vehicle on Days 0–3 and CNO on Days 4–7 in all mice (ABA-mCh; ABA-hM3Dq). **c** While bodyweight change in ABA-mCh and ABA-3Dq mice is comparable on days following vehicle injection (Days 1–4; white background; Days 1–4 $p = 0.885$, $p = 0.280$, $p = 0.949$, $p = 0.277$), ABA-3 Dq, but not ABA-mCh, mice regain bodyweight the day following CNO administration (Days 5-8; grey background; Days 5-8 $p = 0.022$, $p = 0.020$, $p = 0.011$, $p = 0.027$). (d-h) CNO injections in ABA-mCh mice does not alter (**d**) total running (p = 0.859), (**e**) running during food ($p = 0.529$), **f** food anticipatory (**i**, $p = 0.239$), **g** dark cycle ($p = 0.38$), or (**h**) light cycle running ($p = 0.242$), running, while CNO-mediated AgRP activation (Days 4–7) in ABA-3Dq mice decreases (**d**) total ($p = 0.0075$) and (**g**) dark cycle running ($p = 0.0079$), but not (**e**) running during food ($p = 0.163$), **f** food anticipatory ($p = 0.163$), or (**h**) light cycle wheel running ($p = 0.173$), compared to vehicle injected days. **i** Vehicle injections do not alter food intake between ABA-mCh and ABA-3Dq mice on Days 0–3 (Day 0: $p = 0.249$, Day 1: $p = 0.0537$, Day 2: $p = 0.108$, Day 3: $p =$

0.562), whereas CNO administration increases total feeding in ABA-3 Dq mice compared to ABA-mCh controls on the first day of CNO administration (Day 4 $p = 0.042$), but not subsequent days (Day 5: $p = 0.165$, Day 6: $p = 0.091$, Day 7: $p = 0.155$). **j** 15 min binned pellet intake was comparable in response to vehicle injections on Days 0–3 in ABA-mCh and ABA-3Dq mice (top, Day 0: $p = 0.288$, Day 1: $p = 0.479$, Day 2: $p = 0.440$, Day 3: $p = 0.520$). CNO injection increased binned pellet intake on Days 5–7, especially during the first hour of food availability (**j**, bottom (grey)) in ABA-3Dq mice compared to ABA-mCh control mice (Day 5: $t(15)$ $p = 0.034$, $t(45)$ $p = 0.024$, Day 6: $t(30)$ $p = 0.021$, $t(60)$ $p = 0.027$, Day 7: $t(45)$ $p = 0.016$). **k**, **l** Meal size was unaffected by either vehicle ($p = 0.356$) or CNO ($p = 0.843$) injections across groups. **m** Meal number was comparable in response to vehicle injections on Days 0–3 (0.272). **n** CNO injection increased meal number in ABA-3Dq mice compared to ABA-mCh control mice ($p = 0.046$). Significance determined by $p < 0.05$ using a two-way mixed ANOVA followed by Bonferroni post-hoc if appropriate (**c**) a two-way ANOVA followed by Bonferroni post-hoc if applicable (**j**), an unpaired *t*-test (**i**, **k–n**), or a paired *t*-test (**d–h**). ABA-mCh $n = 7$-8, ABA-3Dq $n = 10$-11. Data represented as mean ± SEM. **c**, **j** or as a violin plot with dotted lines at the mean (**d–i**, **k–n**).